

The Contribution of Different Formulation Components on the Aerosol Charge in Carrier-Based Dry Powder Inhaler Systems

Susan Hoe · Daniela Traini · Hak-Kim Chan · Paul M. Young

Received: 2 November 2009 / Accepted: 4 March 2010 / Published online: 31 March 2010
© Springer Science+Business Media, LLC 2010

ABSTRACT

Purpose To measure aerosol performance of a lactose carrier/salbutamol sulphate powder blend and identify contributions of non-formulation and formulation components on the resulting aerosol charge.

Methods A 67.5:1 (%w/w) blend of 63–90 μm lactose with salbutamol sulphate, and lactose alone (with and without the blending process), was dispersed from a Cyclohaler™ into the electrical Next Generation Impactor at 30, 60 and 90 L/min. Mass and charge profiles were measured from each dispersion, as a function of impactor stage. The charge profile from an empty capsule in the Cyclohaler™ was also studied.

Results Lactose deposition from the blend was significantly greater, and net charge/mass ratios were smaller, in the pre-separator compared to formulations without drug. Fine particle fraction of salbutamol sulphate increased with flow rate ($9.2 \pm 2.5\%$ to $14.7 \pm 2.7\%$), but there was no change in net charge/mass ratio. The empty capsule produced a cycle of alternating net positive and negative discharges (~ 200 pC to 4 nC).

Conclusions Capsule charge can ionize surrounding air and influence net charge measurements. Detachment of fine drug during aerosolisation may reduce net specific charge and lead to increased lactose deposition in the pre-separator. Increase in FPF may be due to increased force of detachment rather than electrostatic forces.

KEY WORDS Cyclohaler™ · electrical next generation impactor (eNGI) · electrostatic · lactose · salbutamol sulphate

INTRODUCTION

Treatment of a respiratory disease using dry powder inhalers (DPIs) generally requires the aerosolisation and deposition of small, precise quantities of active pharmaceutical ingredient (API). Large carrier particles may be blended into the dry powder formulation to aid accurate and reproducible dosing as well as improve flow properties. However, in order to effectively deposit fine drug into the respiratory tract, the force of adhesion between the drug and carrier must first be overcome to allow detachment. This adhesion force has been extensively investigated through studies of carrier surface roughness (1,2), carrier material (3), relative humidity (4,5), presence of excipient fines (6–9), carrier particle morphology (8,10,11), API particle morphology (12), carrier surface treatment (6) and other formulation characteristics.

In addition to the aforementioned formulation characteristics, studies have been performed to understand how charge generated from powder formulations and inhalers may influence aerosol performance. In terms of clinical data, little information is available; however, one study reported that the respiratory deposition of monodisperse aerosols of carnauba wax was controlled by the magnitude of aerosol charge (13,14). In addition, computational lung models have indicated charge to be a factor in aerosol deposition in the lower airways (15,16).

In vitro studies into the contact charging (triboelectrification) of dry powder formulations during dispersion have involved an examination of inhaler materials, powder processing procedures, relative humidity, carrier morphology, and operator handling (17–20). However, most of these studies utilise techniques for particle sizing which are unable to detect bipolar charging, such as the Faraday pail and aerosol electrometer (17,18). The electrical low-pressure

S. Hoe · D. Traini · H.-K. Chan · P. M. Young (✉)
Advanced Drug Delivery Group, Faculty of Pharmacy,
The University of Sydney,
Sydney, NSW 2006, Australia
e-mail: paul.young@sydney.edu.au

impactor (ELPI) is the current standard for charge characterisation of pharmaceutical aerosols (19–23). The ELPI is designed to measure aerosol charge distribution corresponding to twelve aerodynamic particle size fractions; however, it is limited to operation at a flow rate of 30 L/min. In addition, use of the vacuum pump causes a spike in electrical signal, demanding dispersions be conducted with air flow already commenced (19,23). Pharmacopoeia convention states that the inhaler must be loaded and in place before air flow is initiated (24,25).

The electrical Next Generation Impactor (eNGI) is a potential replacement for other charge measurement techniques. It is designed as a modification to the architecture of a Next Generation Impactor (NGI), which is listed as Apparatus E in the European Pharmacopoeia (25) and Apparatus 5 and 6 in the United States Pharmacopoeia (24). Unlike the ELPI, it may be operated at a range of flow rates between 30 and 100 L/min. The eNGI has been investigated to assess the electrostatic properties and aerosol performance of single-component pressurised metered dose inhalers (pMDI) and DPI formulations (26–28).

In this current study, the primary aim is to use the eNGI to investigate the tribocharging properties of a lactose carrier-salbutamol sulphate formulation and identify the gelatin capsule and Cyclohaler™ charge contributions to the powder blend. The second objective of this study is to measure the *in vitro* aerosol performance of the binary formulation at a range of flow rates and identify any relationship between powder charge and lung deposition.

MATERIALS AND METHOD

Materials

Lactochem® α -lactose monohydrate was supplied by Friesland Foods Domo (Zwolle, Netherlands). Salbutamol sulphate was obtained from S & D Chemicals (Sydney, Australia). Methanol (Sigma-Aldrich, St Louis, USA) and sodium dodecyl sulphate (Mallinckrodt Baker, New Jersey, USA) were of analytical grade and used as received.

Lactose Carrier Preparation and Decantation

Approximately 450 g of lactose was dry-sieved using a Vibro Retsch sieve shaker (Haan, Germany) and a nest of sieves (Endecotts Ltd., UK). The 63–90 μm sieve fraction was collected and dispersed into absolute ethanol already pre-saturated with lactose. A homogeneous suspension was formed by sonication for 5 min and stirred with a spatula. After allowing lactose carrier particles to settle, the supernatant was decanted and replaced with fresh lactose-saturated

ethanol. This dispersion and decantation process was repeated 8 times, after which the supernatant became clear. The decanted lactose (referred to as lactose through the remainder of the text) was dried in a vacuum oven (Weiss-Gallenkamp, Loughborough, UK) at 65°C and stored in a container with silica gel until required for use.

Salbutamol Sulphate Micronisation

Salbutamol sulphate was micronized with an air jet mill (Trost Air Impact Pulveriser, Trost Equipment Corporation, USA) at a feed pressure of 280 kPa and grinding pressure of 680 kPa.

Particle Size Measurement by Laser Diffraction

The particle size distribution of the lactose was measured by laser diffraction using the Malvern Mastersizer 2000 (Malvern Instruments, Worcestershire, UK) with the Hydro2000SM wet dispersion cell installed. Lactose was added to a small volume sample presentation unit filled with chloroform and dispersed by a dispersion unit controller at a stirrer speed of 2,000 rpm. Particle size analysis (conducted in triplicate) utilised refractive indices of 1.444 for chloroform and 1.533 for lactose. The average geometric particle size distribution of the lactose was $d_{10}=61.63 \mu\text{m}$, $d_{50}=98.66 \mu\text{m}$ and $d_{90}=154.95 \mu\text{m}$, with 1.27% of the powder $\leq 5 \mu\text{m}$. The particle size distribution of micronized SS was also measured using the Mastersizer 2000, but with the Scirocco 2000 dry dispersion unit installed. Using a refractive index of 1.52 and dispersed at 2 bar of pressure in triplicate, the average geometric particle size distribution of SS had $d_{10}=0.805 \mu\text{m}$, $d_{50}=1.734 \mu\text{m}$ and $d_{90}=3.53 \mu\text{m}$.

Preparation of Carrier-Drug Blends

A 67.5:1 (% *w/w*) blend of lactose and micronized salbutamol sulphate (referred to as “lactose-drug blend”) was prepared by geometric hand mixing, transferred to a 20 mL glass vial, and subsequently mixed in a Turbula (Basel, Switzerland) for 15 min at 46 revolutions/min.

The deionisation procedure for blended powders was as follows: A Zerostat 3 anti-static gun (Milty, Hertfordshire, UK) is operated, discharging a stream of positive and negative ions upon the squeeze and release of the trigger. The anti-static gun was discharged ten times to neutralise the powder, which was subsequently stored in a container with silica gel for 1 week to allow for complete charge relaxation.

In addition, a separate portion of lactose (without the addition of drug) was subjected to the same blend, mixing, deionisation and storage procedure as mentioned above (referred to as “blended lactose”).

Scanning Electron Microscopy of Powder Samples

Samples of lactose, blended lactose and lactose-drug blend were mounted onto scanning electron microscopy (SEM) sample stubs and platinum-coated with an Emitech K550X sputter coater (Quorum Emitech, UK), using a voltage of 2 kV and 25 mA current for 2 min. Surface morphology of the particles was analysed using the Zeiss ULTRA plus field emission SEM (Carl Zeiss Inc., USA), at 4 kV voltage. SEM images are presented in Fig. 1.

Electrical Next Generation Impactor

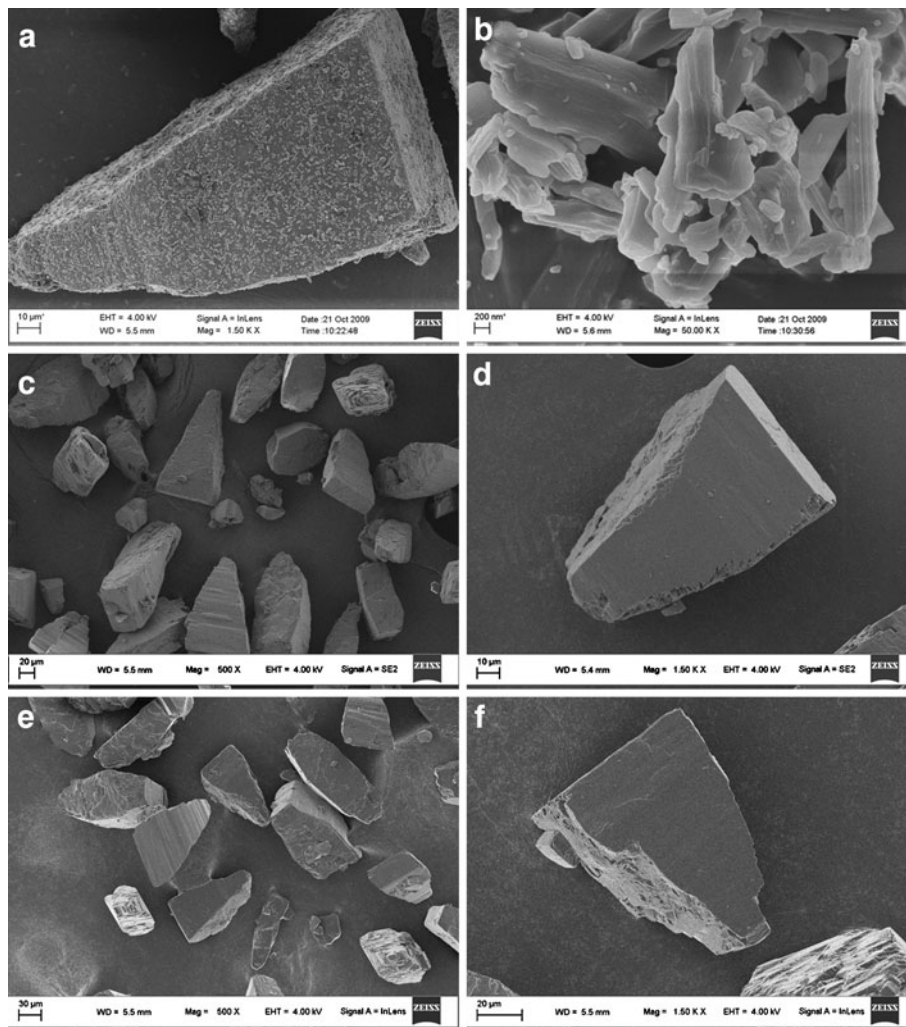
The setup of the electrical Next Generation Impactor (eNGI) in this study (Fig. 2) has been modified from the design outlined in previous publications (27,28) to allow charge measurement from the USP induction port and pre-separator. The eNGI is housed in an earthed metal

enclosure; each collection stage is electrically isolated from neighbouring stages, as well as the impactor body, by PTFE. The induction port, pre-separator and impactor body are electrically isolated from each other by polypropylene adaptors.

All impaction stages, the induction port and pre-separator are in contact with electrometer probes (10 in total), which consist of a BNC-coaxial cable assembly that connects to a Keithley 6517A high resistance/low current electrometer installed with a Model 6521 10-channel scanner card (Keithley Instruments, USA). As a result, each electrometer probe corresponds to a channel. The electrometer operates by measurement of each channel, in sequence (i.e. from USP IP to MOC), completing one “scan” when all 10 channels are measured. A PC collects current-*vs.*-time data from each electrometer channel via RS-232 communication.

The rate at which a scan is completed (“scan speed”) may be adjusted by varying electrometer settings such as

Fig. 1 SEM images (magnifications in parentheses) of **A** lactose-drug blend (1500 \times), **B** micronized salbutamol sulphate (50000 \times), **C** lactose (500 \times), **D** lactose (1500 \times), **E** blended lactose (500 \times) and **F** blended-lactose (1500 \times).



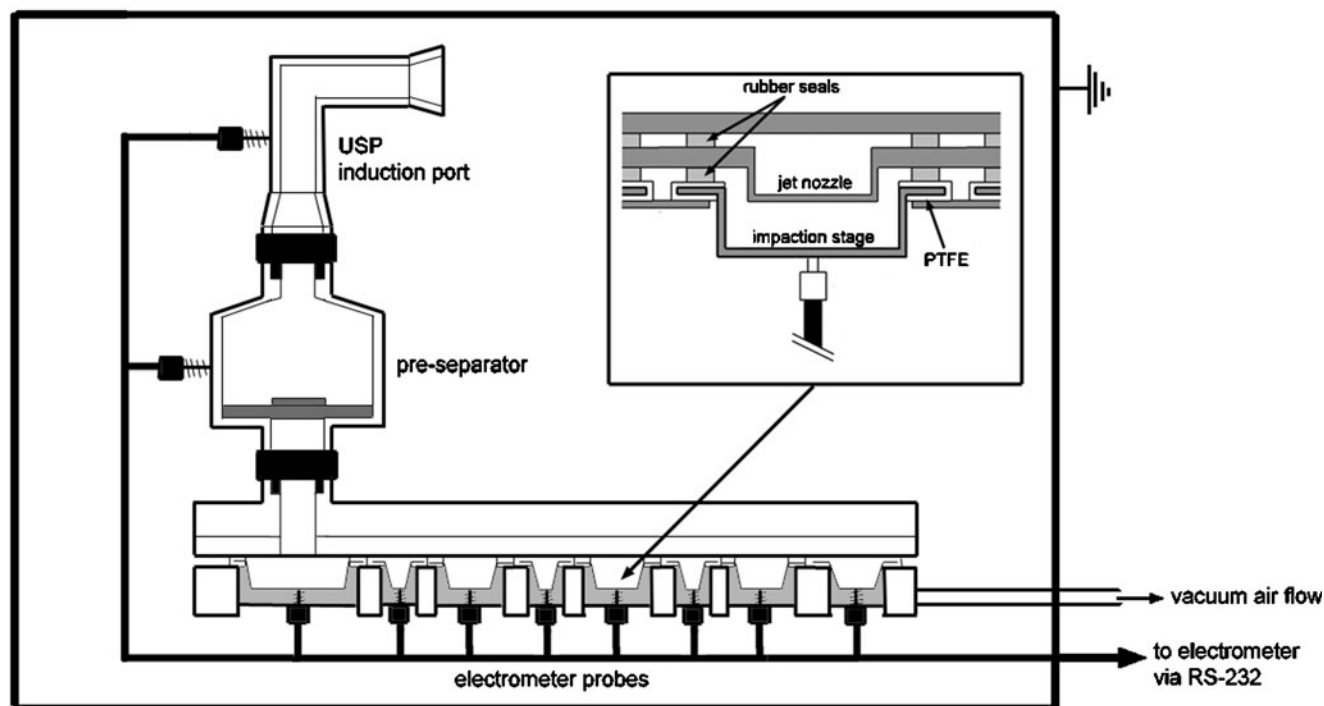


Fig. 2 Schematic diagram of the modified eNGI. Insert: Schematic diagram of an eNGI impaction stage.

analogue-to-digital signal conversion speed, median and averaging filters. Given that average aerosol dispersion is completed within a few seconds under air flow, measurements need to be accomplished as rapidly as possible to maximise resolution. However, the electrometer also needs to contend with very low current when dealing with dry powder aerosols (fine particle charge is usually around the picoamp range), and faster scan speeds result in greater measurement noise. At the fastest scan speed of 4.3 scans/s, noise varies from ± 30 to ± 50 pA, making the distinction of small current-*vs.*-time peaks difficult. Thus, a compromise is required between measurement speed and accuracy; this was found to be at 1 scan/s, equivalent to 0.1 s per channel, which is a measurement speed comparable to that of the ELPI (23)

Pre-measurement Preparations for the eNGI

The electrometer was allowed to warm up for at least 1 hour before operation. Airflow rate through the eNGI was set at the desired value, using a calibrated mass flow meter (TSI Model 4040, TSI Instruments, Germany). Prior to each measurement, the eNGI impaction plates were coated with 1% silicone/hexane (*v/v*) solution and allowed to dry. The Cyclohaler™ was attached to the USP induction port, electrometer baseline was zeroed, and then vacuum airflow was initiated.

Identification of Charge Generated from Gelatin Capsules and the Cyclohaler™

The ability of the eNGI impaction stages to measure current with accuracy and reproducibility has been demonstrated in a previous study (28). However, the eNGI did not include the USP induction port or pre-separator electrometer probe setup. To confirm the capability of accurate current measurement by the induction port and pre-separator, a current study was performed. An MP-3092 power supply (Powertech, Australia) supplying 1.5 V, and $5\text{G}\Omega$ in resistance, was used to apply 0.3 nA current to the induction port and pre-separator. At 0, 30, 60 and 90 L/min, background charge was recorded by the electrometer for 10 s, followed by application and measurement of 0.3 nA current for 10 s.

To assess whether gelatin capsules and/or the Cyclohaler™ provide any contribution to measured charge, an iterative testing procedure was devised, with five procedural steps (Fig. 3). In step A, only the eNGI stages were assembled. In step B, the pre-separator was added to the eNGI and tested, both with and without 20 mL of water. In step C, the induction port was added to the previous setup. In step D, the Cyclohaler™ was inserted into the USP induction port. In step E, an empty gelatin capsule was loaded into the Cyclohaler™ and pierced. At each step, baseline charge (no air-flow) was averaged across

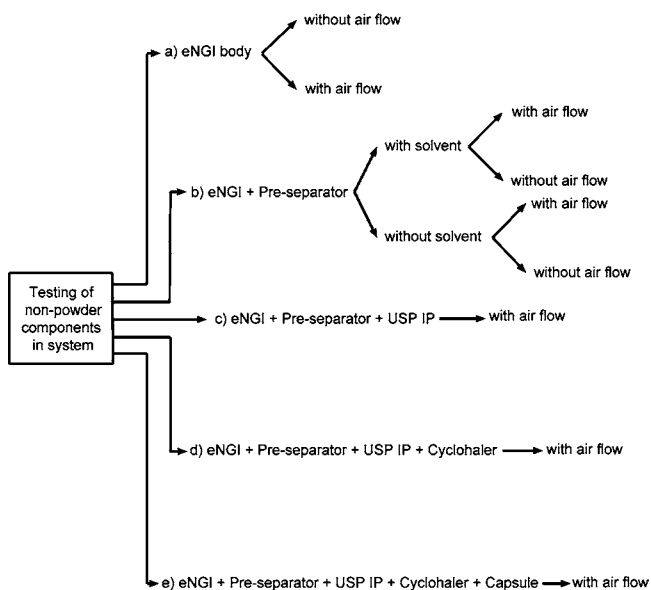


Fig. 3 Testing procedure for assessment of capsule and Cyclohaler™ charge contribution.

all stages for 10 s, and charge measured during airflow (30, 60 and 90 L/min) was also averaged over 10 s. Measurements were carried out in triplicate. After each measurement, in steps D and E, the Cyclohaler™ was deionised with a local area ionizing blower (ION Systems Model 4630, USA) for 2 min.

Investigation of Triboelectrification from Lactose, Blended Lactose and Lactose-Drug Blends

The electrostatic characterisation of lactose, blended lactose and lactose-drug blends was carried out to help identify what contributions lactose carrier and blending procedure have on the net charge of the blend containing drug. The same testing protocol was applied to all three powders. Twenty mL of purified and deionised water was placed in the pre-separator. A size 3 gelatin capsule was filled with the prepared powder (33 ± 1 mg), loaded into the Cyclohaler™, and dispersed into the eNGI at either 30, 60 or 90 L/min, while the eNGI electrometer recorded current-*vs.*-time data. Measurements were carried out in triplicate. For each dispersion, the Cyclohaler™ (including capsule), induction port and eNGI stages were each rinsed with 5 mL of purified and deionised water. These samples, as well as the sample from the pre-separator unit, were assayed by high performance liquid chromatography (HPLC).

High Performance Liquid Chromatography

The HPLC assay was carried out using a Shimadzu Prominence UFLC system, containing an SPD-20A UV-

Vis detector, LC-20AT liquid chromatograph, RID 10A refractive index detector, and SIL-20A HT Autosampler (Shimadzu Corporation, Japan). Detection of salbutamol sulphate required a mobile phase mixture of 60:40 (% *v/v*) methanol:water solution and 1 g/L sodium dodecyl sulphate and Waters Nova-Pak C18 4 μm 3.9 \times 150 mm column (Waters Corporation, Massachusetts, USA). For salbutamol sulphate, the mobile phase flow rate was 1 mL/min, UV detection 276 nm, and injection volume 100 μL . Lactose detection required a mobile phase of 100% deionised water, with a Waters Resolve C18 5 μm 3.9 \times 150 mm (Waters Corporation, Massachusetts, USA). In the case of lactose, the mobile phase flow rate was 1 mL/min, refractive index detection was used, and injection volume was 100 μL .

Dose Content Uniformity of Lactose-Salbutamol Blend

In accordance with pharmacopoeia methodology, ten doses (33 ± 1 mg) of lactose-drug blend were individually assayed by HPLC. The amount of salbutamol sulphate in each dose was within 85 to 115% of the average content.

Data Processing and Statistical Analysis

Current-*vs.*-time data measured from each eNGI electrometer channel, was integrated to give a determination of net charge per stage. Charge/mass data, was calculated by dividing net charge per stage, with total mass (both lactose and salbutamol sulphate) deposited in that stage.

Aerosol performance is generally assessed upon the classification of fine inhalable particles as those with an aerodynamic diameter $< 5 \mu\text{m}$. Fine particle dose is defined as the cumulative mass of drug with a particle size $< 5 \mu\text{m}$ (FPD). In this study, calculation of FPD was carried out in the following manner, according to pharmacopoeia convention (25): for each dispersion, a plot of cumulative mass *vs.* log cut-off diameter was constructed, from which linear regression was used to determine the FPD. From the same linear regression, mass median aerodynamic diameter (MMAD) was calculated, as the particle size at which 50% of the cumulative mass is below this value.

Recovered dose (RD) was defined as the total mass deposited in the eNGI stages, induction port, pre-separator, Cyclohaler™, capsule and adaptor. Emitted dose (ED) entailed the total mass deposited in the eNGI, induction port and pre-separator. Fine particle fraction (FPF) was calculated as the FPD divided by RD. Data was subjected to statistical analysis (SPSS 17.0; SPSS Inc, US), using ANOVA one-way analysis (with Tukey's post-test) to examine for significant difference (defined as $p < 0.05$).

Table 1 Mean Current ($n=10$, St. Dev) Measured in the USP Induction Port and Pre-separator (with Solvent) After the Application of 0.3 nA Current, at 0, 30, 60 and 90 L/min Flow Rate

Flow rate (L/min)	USP induction port		Pre-separator	
	Background (nA)	Applied current (nA)	Background (nA)	Applied current (nA)
0	0.004 (0.005)	0.298 (0.006)	0.002 (0.000)	0.298 (0.008)
30	0.005 (0.002)	0.308 (0.006)	0.002 (0.004)	0.308 (0.012)
60	0.007 (0.003)	0.293 (0.007)	0.001 (0.001)	0.301 (0.007)
90	0.006 (0.002)	0.300 (0.005)	-0.005 (0.002)	0.300 (0.010)

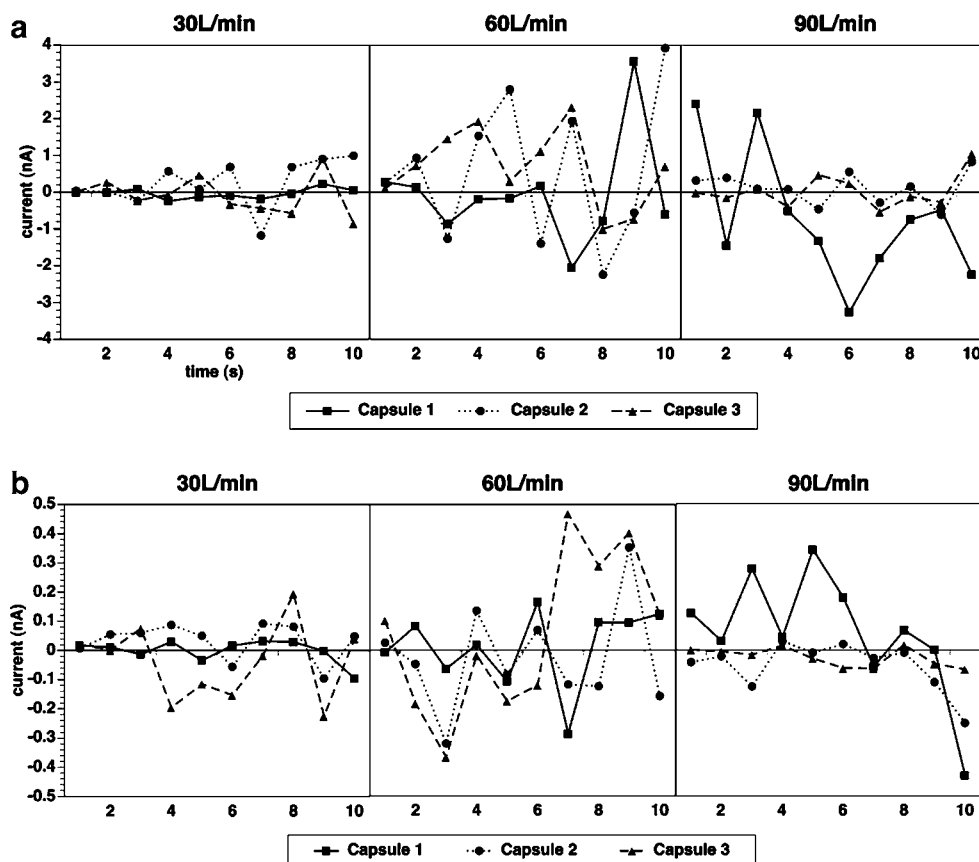
RESULTS

Charge Contribution by Non-formulation Components

Table 1 shows the current measurements recorded by the eNGI after the application of 0.3 nA current to the USP induction port and pre-separator for 10 s at air flow rates of 0, 30, 60 and 90 L/min. The measured current was within ~5% of 0.3 nA, while background noise was <10 pA.

When the eNGI stages, induction port, pre-separator and Cyclohaler™ were successively assembled (Fig. 3, steps A to D), no current-*vs.*-time peaks were observed from any electrometer channel, with or without airflow. The mean net charge (average of net charge across all eNGI components) was <6pC at all flow rates during steps A to D.

Fig. 4 Tribocharging of an empty gelatin capsule within a Cyclohaler™ device, measured in the USP induction port (a) and pre-separator (b). Net current-*vs.*-time plots are shown for three capsules at 30, 60 and 90 L/min.



Net current-*vs.*-time plots in the induction port and pre-separator, for tribocharging from three empty gelatin capsules at 30, 60 and 90 L/min, are shown in Fig. 4. There were no observable relationships between flow rate and net charge, nor was there consistency in charge magnitude from one capsule to the next. However, there is evidence of a cyclic variation in polarity over time within each capsule. Current in the induction port (± 4 nA) was significantly larger than within the pre-separator (± 0.4 nA). Interestingly, no current was detected in the eNGI stages during capsule testing.

Charge Profiles for Lactose, Blended Lactose and Lactose-Drug Blends

The net charge of lactose, blended lactose and lactose-drug blends within the eNGI accessories at 30, 60 and

90 L/min are shown in Table II. For all three powders, charge in the induction port was net positive and net negative in the pre-separator. However, in the USP induction port, individual dispersions were not of a consistent charge polarity for blended lactose (at all flow rates) and for lactose (at 60 L/min). In the pre-separator, all powder dispersions were uniformly net negative across all three flow rates.

In the induction port, an increase in flow rate resulted in an increase in net charge for lactose-drug blend. However, the large variation in charge for blended lactose and lactose prevents the identification of a trend. The net powder charge in the induction port at 30 L/min may be ranked: blended lactose < lactose-drug blend < lactose. There is no trend at 60 or 90 L/min. By comparison, within the pre-separator, all three powders demonstrated an increase in net charge from 30 to 60 L/min, with no further increase at 90 L/min. The net charge in the pre-separator followed the trend: lactose-drug blend < lactose < blended lactose at 30 L/min, and lactose-drug blend < blended lactose = lactose at 60 and 90 L/min.

The net charge results (in nC) were corrected for the total mass deposited (lactose and SS, in μg) in USP induction port and pre-separator, leading to the charge/mass ratio values (Table III). The large variation in net charge reported in the USP induction port is carried over into the net charge/mass ratio results. Although the mean charge/mass ratio appears to increase with flow rate for all three powders, the only distinguishable trend is an increase in charge/mass ratio for lactose-drug blend, from 30 to 60 L/min. Furthermore, the charge/mass ratio of the lactose-drug blend was greater than both lactose samples at 90 L/min and only the blended lactose at 30 and 60 L/min. In the pre-separator, net charge/mass ratio increased from 30 to 60 L/min, and the trend lactose-drug blend < blended lactose = lactose was observed at all three flow rates.

The induction port and pre-separator are designed to capture drug and carrier components which have an aerodynamic size larger than that required for inhalation ($\sim >10 \mu\text{m}$), while the impaction stages may be considered when assessing regional lung deposition. Analysis of the charge distribution across the impaction stages of the eNGI suggested no charge was detected when the decanted or blended lactose were tested at all flow rates.

Fig. 5 depicts the net charge and charge/mass profiles on each impactor stage of the eNGI for the lactose-drug blend at 30, 60 and 90 L/min. As no lactose was detected in the eNGI stages (Mass Deposition Data—Lactose), the charge/mass profiles are based on salbutamol sulphate mass deposition. In general, a bipolar charge distribution was observed, with net negative charge between 2.82–0.34 μm and $>8.06 \mu\text{m}$. Mean net charge appeared to

Table II Net Charge (Mean \pm SD, in nC, $n=3$) of Lactose, Blended Lactose, and Lactose-Drug Blend, Detected in the USP Induction Port and Pre-separator at Aerosolisation Flow Rates of 30, 60 and 90 L/min. The Charge Polarity for Each of the Dispersions is Also Detailed

Powder	Mean net charge (nC)								
	USP induction port			Pre-separator					
	30L/min	60L/min	90L/min	30L/min	60L/min	90L/min	30L/min	60L/min	90L/min
Lactose-drug blend	0.35 \pm 0.14 +, +, +	1.10 \pm 0.54 +, +, +	2.42 \pm 0.77 +, +, +	-0.95 \pm 0.11 -, -, -	-3.78 \pm 0.21 -, -, -	-1.99 \pm 0.63 -, -, -			
Blended lactose	0.01 \pm 0.03 -, +, -	0.10 \pm 0.14 -, +, +	1.00 \pm 1.81 -, +, +	-5.62 \pm 0.53 -, -, -	-9.06 \pm 5.04 -, -, -	-8.45 \pm 3.64 -, -, -			
Lactose	1.11 \pm 0.34 +, +, +	-0.24 \pm 3.72 -, -, +	4.60 \pm 1.61 +, +, +	-3.46 \pm 0.98 -, -, -	-10.10 \pm 4.20 -, -, -	-9.52 \pm 4.34 -, -, -			

Table III Net Charge/Mass Ratio (Mean \pm SD, nC/ μ g, $n=3$) of Lactose, Blended Lactose, and Lactose-Drug Blend, Detected in the USP Induction Port and Pre-separator at Aerosolisation Flow Rates of 30, 60 and 90 L/min

Powder	Net charge/mass ratio (nC/ μ g)					
	USP induction port			Pre-separator		
	30L/min	60L/min	90L/min	30L/min	60L/min	90L/min
Lactose-drug blend	0.100 \pm 0.062	0.744 \pm 0.372	2.294 \pm 1.276	-0.035 \pm 0.005	-0.135 \pm 0.014	-0.067 \pm 0.019
Blended lactose	0.002 \pm 0.006	0.016 \pm 0.025	0.250 \pm 0.514	-0.279 \pm 0.030	-0.431 \pm 0.224	-0.347 \pm 0.180
Lactose	0.096 \pm 0.002	0.013 \pm 0.562	0.640 \pm 0.356	-0.188 \pm 0.018	-0.454 \pm 0.205	-0.364 \pm 0.159

increase with flow rate; however, wide error bars resulted in overlap between 60 and 90 L/min profiles. Charge/mass profiles showed an overlap between all three flow rates.

Mass Deposition Data—Lactose

Table IV reports the mass deposition of lactose from each formulation in the Cyclohaler™, induction port and pre-separator at 30, 60 and 90 L/min. For the lactose in the drug blend, the vast majority was deposited in the pre-separator unit (~28 mg). For this formulation, lactose deposition in the induction port and Cyclohaler decreased with increased flow rate.

In comparison, the mass of the decanted lactose alone was more evenly distributed between the induction port (11.59 \pm 3.67 mg) and pre-separator (18.20 \pm 3.31 mg) at 30 L/min. However, as flow rate increased, deposition shifted towards the pre-separator (22.59 \pm 1.77 mg at 60 L/min increasing to 26.1 \pm 0.49 mg at 90 L/min). For the blended lactose, the majority was deposited in the pre-separator at 30 L/min with deposition decreasing in the induction port with increased flow rate. No lactose was detected in the eNGI stages.

One-way ANOVA (Tukey's post test) was used to compare deposition of lactose between formulations within

each eNGI accessory. Significant differences ($p < 0.05$) in mean deposition were found between the formulations (lactose, blended lactose and lactose-drug blends).

Mass Deposition Data—Salbutamol Sulphate

Fig. 6 presents the mass deposition of salbutamol sulphate in the eNGI after aerosolization at 30, 60 and 90 L/min. The insert illustrates the particle size distributions at the aforementioned flow rates, based upon the aerodynamic cut-off diameters determined for each of the seven eNGI impaction stages (24,25). The micro-orifice collector (MOC) is not designed to be an impactor stage and, consequently, cannot be included in particle sizing data (29).

At 30 L/min, coarse or undetached salbutamol sulphate particles were evenly divided between the induction port (142.8 \pm 21.8 μ g) and pre-separator (192.3 \pm 25.8 μ g). With an increase in flow rate to 60 L/min, deposition shifted towards the pre-separator (284.2 \pm 16.6 μ g). Further increase to 90 L/min resulted in no further change in induction port or pre-separator deposition; however, over this range, device retention dropped significantly.

In vitro aerosol parameters (ED, FPD, RD, FPD, MMAD) calculated from salbutamol sulphate mass deposition data are shown in Table V. In general, as flow rate increased, an increase in FPD and FPF and decrease in

Fig. 5 Net charge (left) and net charge/mass (right) profiles for salbutamol-lactose blend, dispersed from a Cyclohaler™ (using the USP induction port and pre-separator unit) at 30, 60 and 90 L/min.

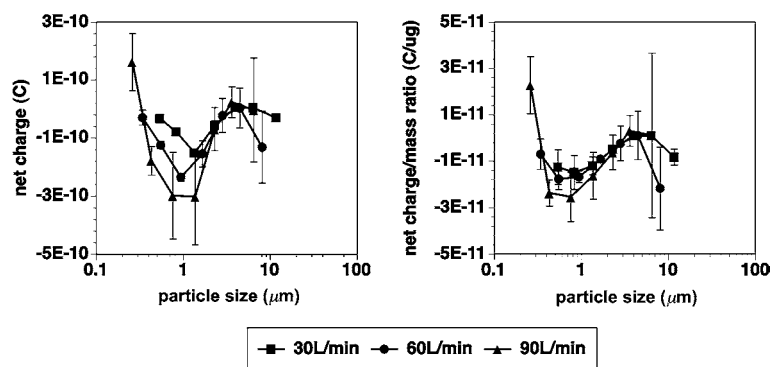


Table IV Mean (S.D) Mass Deposition of Lactose from B_{LAC-SS} , L_B and L_D , in the Cyclohaler™, USP Induction Port and Pre-separator at Aerosolisation Flow Rates of 30, 60 and 90 L/min ($n=3$)

		Lactose mass (mg)		
		Lactose-drug blend	Blended lactose	Lactose
30 L/min	Cyclohaler	0.390 (0.209)	0.773 (0.171)	0.939 (0.362)
	Contact electrification	4.099 (2.123)	7.745 (2.106)	11.589 (3.663)
	Contact electrification	27.133 (1.495)	20.373 (3.481)	18.203 (3.311)
60 L/min	Cyclohaler	0.255 (0.021)	0.139 (0.043)	0.667 (0.493)
	USP induction port	1.463 (0.145)	3.764 (0.663)	7.132 (0.893)
	Pre-separator	27.892 (1.434)	24.869 (3.586)	22.594 (1.739)
90 L/min	Cyclohaler	0.174 (0.030)	0.120 (0.018)	0.150 (0.007)
	USP induction port	1.156 (0.494)	4.130 (2.379)	7.713 (1.423)
	Pre-separator	29.252 (3.241)	25.022 (1.907)	26.052 (0.490)

MMAD were observed (e.g. FPF increased from 9.2 ± 2.5 to $14.7 \pm 2.7\%$, while MMAD decreased from 2.0 ± 0.3 to $1.4 \pm 0.1 \mu\text{m}$ between 30 L/min and 90 L/min, respectively).

DISCUSSION

Charge Developed by Aerosolizing Empty Gelatin Capsules at Different Flow Rates

During the current measurement tests carried out on the induction port and pre-separator (Charge Contribution by Non-formulation Components, Table I), background

noise was kept low ($<10 \text{ pA}$) while the 0.3 nA current applied to each section was measured to within 5% of that value. This demonstrates that the electrometer probes connected to the USP induction port and pre-separator in this study are capable of accurate and reproducible measurement of current, both with and without airflow. Furthermore, the successive assembly of induction port, pre-separator and Cyclohaler™ (Fig. 3, steps A to D) did not result in any detected charge under air flow. Thus, this modified eNGI setup is appropriate for characterising aerosol charge.

As there was no charge detected during steps A to D, the charge detected at step E (eNGI, pre-separator, USP induction port, Cyclohaler™ and capsule, Fig. 4) may be attributed to the gelatin capsule alone. However, as the capsule was empty, the induction port and pre-separator were essentially measuring charge in air. One possible cause for this observation is ionization of the air molecules. Airflow through the Cyclohaler™ initiates capsule oscillation, which results in tribocharging of the capsule and inhaler surfaces. Charge density accumulates until it is high enough to ionize the air molecules surrounding the surface—approximately 1 nC/cm^2 (30). In this study, net charge in air ranges from $\sim 200 \text{ pC}$ to $>4 \text{ nC}$ (Fig. 4), which gives an indication that surface charge on the capsule and Cyclohaler™ is sufficient to ionise the air.

The oscillation in capsule current-*vs.*-time profiles appears to be a cycle of net negative and positive discharges in air. One possible scenario is the existence of positively and negatively charged regions within each surface, whose magnitudes can vary with surface impurities, deformation or uneven contact. As a result, the net charge in air can vary depending on which polarity dominates. Another possibility is variation in the net charge contribution by capsule and Cyclohaler™ surfaces towards air ionization. However, the measurement of dynamic charge at the capsule surface, as well as the determination of contact

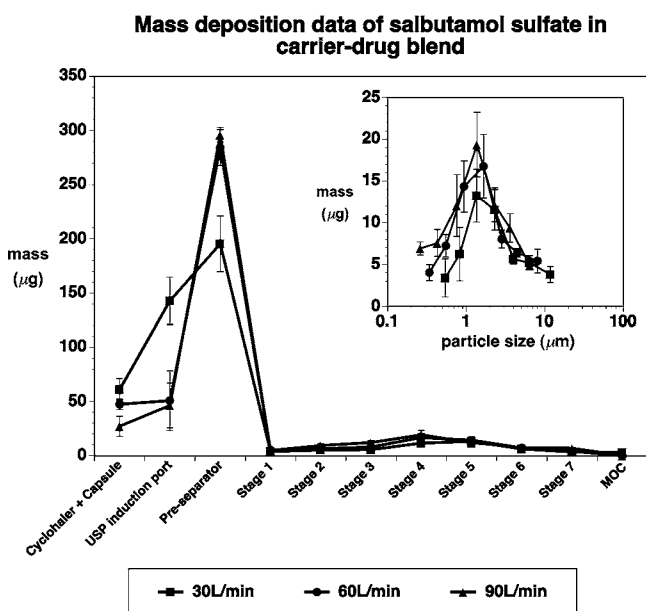


Fig. 6 Mass deposition data of salbutamol sulphate from 1:67.5 (%w/w) lactose-drug blend in eNGI, at aerosolisation flow rate of 30, 60 and 90 L/min. Insert: Mass deposition in eNGI impaction stages, corrected for aerodynamic cut-off.

Table V Mean *In Vitro* Aerosol Parameters Calculated for Salbutamol Sulphate Dispersed by a Cyclohaler™ DPI Device, from a Lactose-Drug Blend at Aerosolisation Flow Rates of 30, 60 and 90 L/min ($n=3$, St.Dev)

Flow rate (L/min)	ED (μg)	FPD (μg)	RD (μg)	FPF (%)	MMAD (μm)
30	390.1 (24.5)	41.7 (13.1)	451.2 (20.1)	9.2 (2.5)	2.1 (0.3)
60	397.4 (22.2)	55.9 (11.6)	444.8 (26.0)	12.5 (1.8)	1.6 (0.1)
90	414.9 (13.9)	65.2 (13.3)	442.0 (12.0)	14.7 (2.7)	1.4 (0.1)

ED emitted dose, FPD fine particle dose, RD recovered dose, FPF fine particle fraction, and MMAD mass median aerodynamic diameter

area during triboelectrification, is problematic. At this point in time, it is difficult to quantify surface charge density.

The charge detected in the pre-separator unit is approximately one-tenth the magnitude of that which was detected in the upstream induction port, while no charge was detected in the eNGI stages. This is likely to be due to the majority of ionized gas molecules interacting with the USP induction port surface under turbulence, with the remainder interacting with the pre-separator components.

Charge and Mass Profiles in the Induction Port and Pre-separator

As mentioned in “Investigation of Triboelectrification from Lactose, Blended Lactose and Lactose-Drug Blends” section, the charge characterisation of lactose and blended lactose was performed to identify what contributions lactose carrier and blending procedure have on the tribocharging of lactose-salbutamol sulphate blends. In the pre-separator, the lactose-drug blend’s charge-to-mass ratio was significantly less than for both lactose and blended lactose at all flow rates ($p<0.05$; Table III). However, lactose deposition for the lactose-drug blend was greater (26–32 mg) when compared to lactose alone (~5–27 mg). Meanwhile, in the induction port, the lactose deposition from the lactose-drug blend (1–6 mg) was less than lactose (6–14 mg) or blended lactose (Table IV).

In the “Charge Contribution by Non-formulation Components” section it was reported that capsule-induced current in air oscillated between +4 nA and -4 nA in the USP induction port. The magnitude and inconsistency of this current has implications for the net charge measurements in the USP induction port. The polarity of individual dispersions documented in Table II shows a similar inconsistency within the USP induction port, resulting in mean net charges with variations in excess of 100% (blended lactose at all flow rates, lactose at 60 L/min). This indicates that the charge measured in the induction port may not just be the result of inter-particle, particle-capsule and particle-inhaler collision, but also the result of capsule-induced current in air. Although the dispersions of lactose-drug blend were uniformly net positive, it is difficult to identify what influence capsule-

induced current has on these measurements. In comparison, capsule-induced current in air oscillated between +0.4 nA and -0.4 nA in the pre-separator and is expected to have less of an influence on net charge measurements in this region. Consequently, all dispersions produced net negative charge in the pre-separator.

Fig. 1A shows that the surface of the lactose carrier particle is covered in fine particulates, of which the majority may be assumed to be drug. It is likely that it is this drug, which engages in tribocharging with other fine particles and inhaler surfaces during the aerosolisation process. A portion of these fine drug particles detach during aerosolisation, leaving the lactose carrier and undetached salbutamol sulphate particulates with a lower net specific charge. The charge/mass ratio of lactose-drug blend is significantly smaller in the pre-separator than lactose and blended lactose (Table II) at all flow rates, supporting this proposition. A lower specific charge points towards a reduction in agglomeration and adhesion via electrostatic forces, resulting in a greater proportion of lactose collected in the pre-separator compared with lactose alone.

The effect of the blending procedure on net charge and mass deposition in the induction port and pre-separator is borne out in the results of blended lactose sample dispersion in the eNGI. The net charge/mass ratio of blended lactose is similar to unblended lactose (Table III). Meanwhile, the actual mass of blended lactose deposited in the induction port and pre-separator sits between unblended lactose and lactose-drug blends (Table IV). This suggests that the low-shear mixing procedure employed in production of a blend does not significantly affect specific charge of the powder, but may aid the breakdown of large aggregates and increase deposition of lactose carrier in the pre-separator.

While net charge and charge/mass ratio results in the pre-separator have provided some useful information about the influence of fine drug detachment and blending on coarse particle charge and deposition, the issue of large charge variation in the USP induction port indicates that the eNGI and any other impactor-based electrostatic characterisation techniques may encounter difficulties resolving the charge carried by the aerosolised powder, from the capsule-induced current in air.

Mass and Charge Profiles of Fine SS Particles

Studies available in literature that have looked at the aerosol performance of lactose-salbutamol blends, have typically employed lactose carrier particles, which have not been decanted. Fines have been suggested to improve aerosolisation efficiency of drug by filling “active sites” on lactose carrier surfaces, thereby reducing the adhesion force of drug to carrier and enhancing detachment under inhalational airflow (8,31,32). Traini *et al.* (2008) and Young *et al.* (2007) dispersed untreated lactose-salbutamol sulphate blend (67.5:1) into the NGI at 60 L/min (FPD <4.46 μm) with the use of a Cyclohaler™, and reported FPF values between 17% and 20%, significantly greater than the FPF in this current study, in which decanted lactose was employed ($12.5 \pm 1.8\%$) (4,33). The results give some support to the assertion that addition of fines improve aerosol performance.

With regards to the fine particle charge (Fig. 5), the charge profiles were mostly unipolar negative, which is in agreement with numerous studies of micronized SS dispersion from DPIs (4,17,20). Looking at the relationship between flow rate and net charge profiles, net charge appears to increase with flow rate, although the wide error bars lead to overlap between adjacent plots. However, net charge/mass ratio profiles show an even greater overlap across all three flow rates; this indicates that the charge per fine particle does not change with flow rate. Meanwhile, FPD and ED both slightly increased with flow rate. As a result, the increase in FPF from 30 to 90 L/min ($9.2 \pm 2.5\%$ to $14.7 \pm 2.7\%$) is more likely to be due to increased detachment force in turbulent air rather than the influence of electrostatic forces. This is in contrast with the net charge results in the induction port and pre-separator, which suggested that lactose carrier deposition was affected by electrostatic forces.

CONCLUSIONS

The rapid oscillation of a gelatin capsule in the Cyclohaler™ DPI may generate a surface charge density great enough to ionize the surrounding air, detectable in the USP induction port and pre-separator. Consequently, the net charge measured in these regions may be affected by this phenomenon—dispersed powder may be charged by ionized air or contact with capsule and Cyclohaler™ surfaces.

The detachment of salbutamol sulphate from lactose carrier particles during aerosolisation may leave the remaining lactose and undetached salbutamol with a lower net specific charge compared to dispersed lactose carrier alone. This, in turn, can reduce agglomeration and adhesion induced by electrostatic forces and result in the

shift in lactose deposition from USP induction port to pre-separator. The blending procedure was not found to affect powder charge, but may increase deposition of lactose carrier in the pre-separator by breaking down aggregates.

In terms of aerosol performance, there was an increase in fine particle dose, emitted dose, and fine particle fraction with flow rate. This was attributed to improved detachment of drug from carrier particle in turbulent air. The lack of change in charge/mass ratio with flow rate indicated that electrostatic charge did not play an influential part in aerosolisation efficiency, in this case.

Although this study endeavoured to isolate sources of triboelectrification (capsule/Cyclohaler™, lactose carrier, blending procedure), ultimately the influences of these factors are not strictly additive, underlining the complexities in the tribocharging of binary dry powder formulations. Future studies may require the employment of computer modelling (e.g. discrete element modelling or computational fluid dynamics) in conjunction with the eNGI as an *in vitro* method of aerosol performance testing for further understanding of aerosol charging.

ACKNOWLEDGEMENTS

The authors would like to thank GlaxoSmithKline Australia for the provision of a postgraduate support grant, and Dr. Handoko Adi for assistance with SEM imaging.

REFERENCES

1. Islam N, Stewart P, Larson I, Hartley P. Surface roughness contribution to the adhesion force distribution of salmeterol xinafoate on lactose carriers by atomic force microscopy. *J Pharm Sci.* 2005;94:1500–11.
2. Young PM, Kwok P, Adi H, Chan H-K, Traini D. Lactose composite carriers for respiratory delivery. *Pharm Res.* 2009;26:802–10.
3. Harjunen P, Lankinen T, Salonen H, Lehto V-P, Järvinen K. Effects of carriers and storage of formulation on the lung deposition of a hydrophobic and hydrophilic drug from a DPI. *Int J Pharm.* 2003;263:151–63.
4. Young PM, Sung A, Traini D, Kwok P, Chiou H, Chan H-K. Influence of humidity on the electrostatic charge and aerosol performance of dry powder inhalers carrier-based systems. *Pharm Res.* 2007;24:963–70.
5. Lohrmann M, Kappl M, Butt H-J, Urbanetz NA, Lippold BC. Adhesion forces in interactive mixtures for dry powder inhalers—evaluation of a new measuring method. *Eur J Pharm Biopharm.* 2007;67:579–86.
6. Zeng XM, Martin GP, Marriott C, Pritchard J. Lactose as a carrier in dry powder formulations: the influence of surface characteristics on drug delivery. *J Pharm Sci.* 2001;90:1424–34.
7. Islam N, Stewart P, Larson I, Hartley P. Effect of carrier size on the dispersion of salmeterol xinafoate from interactive mixtures. *J Pharm Sci.* 2004;93:1030–8.

8. Tee SK, Marriott C, Zeng XM, Martin GP. The use of different carriers as fine and coarse carriers for aerosolised salbutamol sulphate. *Int J Pharm.* 2000;208:111–23.
9. Adi H, Larson I, Chiou H, Young P, Traini D, Stewart P. Role of agglomeration in the dispersion of salmeterol xinafoate from mixtures for inhalation with differing drug to fine lactose ratios. *J Pharm Sci.* 2007;97:3140–52.
10. Zeng XM, Martin GP, Marriott C, Pritchard J. The effects of carrier size and morphology on the dispersion of salbutamol sulphate after aerosolization at different flow rates. *J Pharm Pharmacol.* 2000;52:1211–21.
11. Zeng XM, Martin GP, Marriott C, Pritchard J. The influence of carrier morphology on drug delivery by dry powder inhalers. *Int J Pharm.* 2000;200:93–106.
12. Adi H, Traini D, Chan H-K, Young PM. The influence of drug morphology on aerosolisation efficiency of dry powder inhaler formulations. *J Pharm Sci.* 2007;97:2780–8.
13. Melandri C, Tarroni G, Prodi V, de Zaiacomo T, Formignani M, Lombardi CC. Deposition of charged particles in the human airways. *J Aerosol Sci.* 1983;14:657–69.
14. Prodi V, Mularoni A. Electrostatic lung deposition experiments with humans and animals. *Ann Occup Hyg.* 1985;29:229–40.
15. Bailey AG, Hashish AH, Williams TJ. Drug delivery by inhalation of charged particles. *J Electrostat.* 1998;44:3–10.
16. Balachandran W, Machowski W, Gaura E, Hudson C. Control of drug aerosol in human airways using electrostatic forces. *J Electrostat.* 1997;40 & 41:579–84.
17. Byron PR, Peart J, Staniforth J. Aerosol electrostatics I: properties of fine powders before and after aerosolisation by dry powder inhalers. *Pharm Res.* 1997;14:698–705.
18. Chow KT, Zhu K, Tan RBH, Heng PWS. Investigation of electrostatic behavior of a lactose carrier for dry powder inhalers. *Pharm Res.* 2008;25:2822–34.
19. Kwok PCL, Chan H-K. Effect of relative humidity on the electrostatic charge properties of dry powder inhaler aerosols. *Pharm Res.* 2008;25:277–88.
20. Telko MJ, Kujanpää J, Hickey AJ. Investigation of triboelectric charging in dry powder inhalers using electrical low pressure impactor (ELPI). *Int J Pharm.* 2007;336:352–60.
21. Crampton M, Kinnersley R, Ayres J. Sub-micrometer particle production by pressurised metered dose inhalers. *J Aerosol Med.* 2004;17:33–42.
22. Glover W, Chan H-K. Electrostatic charge characterization of pharmaceutical aerosols using electrical low-pressure impactor (ELPI). *J Aerosol Sci.* 2004;35:755–64.
23. Keskinen J, Pietarinen K, Lehtimäki M. Electrical low pressure impactor. *J Aerosol Sci.* 1992;23:353–60.
24. Chapter <601>. United States Pharmacopoeia 31—National Formulary 26, United States Pharmacopoeial Convention Inc., 2008.
25. Section 2.9.18—Appendix XII C. Consistency of formulated preparations for inhalation., British Pharmacopoeia, Vol. IV, 2009.
26. Hoe S, Traini D, Chan H-K, Young P. The influence of flow rate on the aerosol deposition profile and electrostatic charge of single and combination metered dose inhalers. *Pharm Res.* 2009;26:2639–46.
27. Hoe S, Traini D, Chan H-K, Young PM. Measuring charge and mass distributions in dry powder inhalers using the electrical Next Generation Impactor (eNGI). *Eur J Pharm Sci.* 2009;38:88–94.
28. Hoe S, Young PM, Chan H-K, Traini D. Introduction of the electrical Next Generation Impactor (eNGI) and investigation of its capabilities for the study of pressurized metered dose inhalers. *Pharm Res.* 2009;26:431–7.
29. Marple VA, Roberts DL, Romay FJ, Miller NC, Truman KG, van Oort M *et al.* Next generation pharmaceutical impactor (a new impactor for pharmaceutical inhaler testing). Part I: design. *J Aerosol Med.* 2003;16:283–99.
30. Lowell J, Rose-Innes AC. Contact electrification. *Adv Phys.* 1980;29:947–1023.
31. Zeng XM, Martin GP, Tee S-K, Marriott C. The role of fine particle lactose on the dispersion and deaggregation of salbutamol sulphate in an air stream *in vitro*. *Int J Pharm.* 1998;176:99–110.
32. Young PA, Edge S, Traini D, Jones MD, Price R, El-Sabawi D *et al.* The influence of dose on the performance of dry powder inhalation systems. *Int J Pharm.* 2005;296:26–33.
33. Traini D, Young PM, Thielmann F, Acharya M. The influence of lactose pseudopolymorphic form on salbutamol sulfate-lactose interactions in DPI formulations. *Drug Dev Ind Pharm.* 2008;34:992–1001.